



Project on Visualize the Shock Structures from a CD Nozzle

¹Meharban Alam, ²Dr. Mohammad Zunaid

¹M. Tech. Scholar, Department of Mechanical Engineering, Delhi Technological University, Delhi, India¹

²Professor, Department of Mechanical Engineering, Delhi Technological University, Delhi, India²

Abstract

The project titled “*Visualize the Shock Structures from a CD Nozzle*” focuses on the study and visualization of compressible flow phenomena occurring inside and outside a Convergent-Divergent (CD) nozzle under different pressure conditions. In high-speed aerodynamic applications, shock waves are formed due to sudden changes in pressure, temperature, and velocity when the flow reaches supersonic conditions. The objective of this project is to analyze the formation of normal and oblique shock structures in a CD nozzle using computational and visualization techniques. The study examines variations in Mach number, pressure ratio, density, and velocity distribution throughout the nozzle section. Different flow regimes such as subsonic flow, choked flow, over-expanded flow, under-expanded flow, and perfectly expanded flow are investigated to understand the behavior of shock waves. The project employs simulation tools and fluid dynamics principles to generate graphical representations of pressure contours, Mach contours, and shock patterns. The obtained results help in understanding the aerodynamic performance and efficiency of nozzles used in aerospace propulsion systems, jet engines, rockets, and supersonic applications. The visualization of shock structures provides better insight into compressible fluid flow behavior and contributes to the design optimization of high-speed propulsion devices.

Keywords: CD Nozzle, Shock Waves, Compressible Flow, Supersonic Flow, Mach Number, Flow Visualization

I. INTRODUCTION

Compressible flow refers to fluid motion in which the density of the fluid changes significantly due to variations in pressure or velocity. When the density differs by more than 5% from the stagnation density, the flow is treated as compressible. Such effects become important when the Mach number exceeds approximately 0.3.

According to the local Mach number (M), compressible flow is classified into four regions: $M \leq 0.8$ – Subsonic flow

$0.8 \leq M \leq 1.2$ – Transonic flow $M > 1$ – Supersonic flow

$M > 5$ – Hypersonic flow

A nozzle is a device used to increase the velocity of a fluid and to control its direction by converting pressure energy into kinetic energy. The convergent–divergent or de Laval nozzle, invented in 1890 by Swedish engineer Karl Gustaf Patrik de Laval, is capable of accelerating the flow to supersonic speed.

In a convergent nozzle, the cross-sectional area decreases from inlet to outlet, which increases the fluid velocity while keeping the mass flow rate constant. In a de Laval nozzle, the

convergent part accelerates the subsonic flow to Mach 1, and the divergent part further accelerates it to supersonic speeds.

When the inlet pressure and exit pressure are not perfectly matched, different shock wave patterns appear inside or outside the nozzle. A shock wave is a thin region where fluid properties such as pressure, temperature, and velocity change abruptly. Shock waves typically move faster than the local speed of sound. In gas dynamics, common shock types include normal shocks and oblique shocks.

Normal Shock Waves

A normal shock is formed when a supersonic flow is forced to slow down to subsonic speed within a very thin region that is perpendicular to the direction of flow. Across this shock layer, the pressure and temperature increase suddenly, while the flow velocity drops sharply. In a convergent–divergent nozzle, normal shocks commonly appear in the diverging section when the back pressure becomes higher than the nozzle’s operating or design pressure.

Oblique Shock Waves

Oblique shocks develop at an angle to the flow direction and may occur in both the convergent and divergent parts of a nozzle. These shocks are weaker compared to normal shocks and produce smaller changes in the flow properties. Oblique shocks are typically observed when the back pressure is lower than the value that would produce a normal shock, but still higher than the ideal design condition.

Underexpanded Flow

Underexpanded flow occurs when the pressure at the nozzle exit is greater than the surrounding atmospheric pressure ($P_{\text{exit}} > P_{\text{atm}}$). After leaving the nozzle, the jet continues to expand, forming expansion fans and Mach waves as it adjusts toward the ambient pressure. This expansion continues until the jet pressure becomes equal to the outside pressure.

Overexpanded Flow

Overexpanded flow happens when the exit pressure of the nozzle is lower than the ambient pressure ($P_{\text{exit}} < P_{\text{atm}}$). In this case, the jet tries to expand after exiting the nozzle, but the surrounding air compresses it back, creating shock waves just outside the nozzle.

When the flow reaches Mach 1 at the throat, the nozzle is said to be choked, meaning that further decreases in back pressure cannot increase the mass flow rate. For ideal performance, the nozzle should operate with an exit pressure equal to the ambient pressure. The pressure ratio between the inlet and exit governs where shock waves form and how strong they are.

II. LITERATURE REVIEW

The exit section of a convergent–divergent (C–D) nozzle typically experiences the lowest pressure and mass flow rate due to the rapid acceleration and expansion of the flow. The behavior of real fluids is influenced by viscosity, which represents the fluid’s natural resistance to deformation and affects both liquids and gases at the molecular level.

Flows occurring over bodies without confinement, such as projectiles, plates, cylinders, spheres, and airfoils, are categorized as external flows. In such problems, viscous effects are mainly limited to the boundary layer formed on the surface. Internal flows, in contrast, are restricted within passages or ducts where viscosity has a wider influence on the overall flow field.

A convergent–divergent nozzle is essential for generating supersonic airflow, as purely convergent nozzles cannot accelerate the flow beyond Mach 1 without a diverging section. Depending on the geometry, fluid motion may be analyzed as one-dimensional, two-dimensional, or three-dimensional. Although real flows are inherently three-dimensional, they are often simplified to lower-dimensional models to reduce computational effort. The governing principles for these analyses rely on the conservation of mass, momentum, and energy.

Several studies have examined the flow behavior downstream of a C–D nozzle connected to a sudden expansion duct. Experimental investigations have measured wall pressure and base pressure to understand methods of controlling base drag. One-dimensional flow assumptions are commonly used to model situations where significant flow variations occur primarily along a single direction.

In earlier research, ducts with a diameter-to-height ratio of 1.6 and a length of 10D were tested. Flow characteristics were analyzed at various nozzle exit Mach numbers, including 1.87, 2.2, and 2.58. Numerical simulations were also performed over a wide range of nozzle pressure ratios (NPR) from 3 to 11. The $k-\epsilon$ turbulence model was frequently employed for these simulations. Later studies extended the analysis using ANSYS to evaluate the effect of NPR, Mach number, and geometric ratios on shock formation and expansion waves. Additional computational work has also explored the flow field around wedges using similar numerical approaches.

In the present work, the nozzle geometry corresponds to a design Mach number of 2. The inlet and outlet boundaries are defined using pressure inlet and pressure outlet conditions. For NPR = 6.82, the inlet pressure is set to 691036.5 Pa with an inlet temperature of 300 K, while the outlet pressure is maintained at 101325 Pa. To examine underexpanded shock structures, an additional simulation is performed at NPR = 12.25 with an inlet pressure of 490000 Pa and an outlet pressure of 40000 Pa. The resulting shock waves and flow features are visualized through contour plots.

III. METHODOLOGY

3.1 Geometrical Modelling

The goal of the current study is to apply a transient compressible stream via a two-dimensional C–D nozzle using the CFD approach. However, ANSYS technologies are used to optimize several aspects including density-based implicit solver, NPR, Mach number, etc. All the dimensions are given in Table 1.

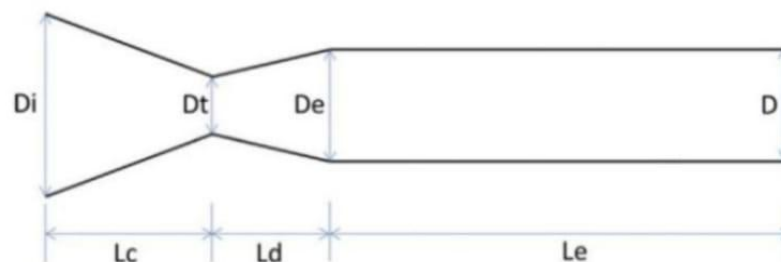


Figure 1: Nozzle with Enlarged Duct

The early findings from the CFD simulations were used to accomplish the following study objectives: In ANSYS, the C–D nozzle modelling was carried out smoothly. The symbol for each section is shown in Fig 1. The lines are initially created and subsequently connected according to the design concept.

Table 1: Details of C–D Nozzle for Mach Number, M = 2

Segmen	Mach Number = 2
Inlet diameter (D _i)	25.9 mm
Throat diameter (D _t)	7 mm
Exit diameter (D _e)	10 mm
Convergent length (L ^c)	25 mm
Divergent length (L ^d)	13.2 mm
Extended length (L _e)	60 mm
Convergent angle (A ^c)	20 degree
Divergent angle (A ^d)	5 degree

The surface from the sketching option was used to generate the 2D surface that is seen in Fig 2.



Figure 2: Two-dimensional CFD model of the nozzle for Mach number 2

3.2 Governing Equations

The governing equations of fluids consist of:

Continuity equation:

$$\left(\frac{\partial \rho}{\partial t}\right) + \left(\frac{\partial(\rho u_i)}{\partial x_i}\right) = 0 \tag{1}$$

Momentum equation:

$$\left(\frac{\partial(\rho u_i)}{\partial t}\right) + \left(\frac{\partial(\rho(u_j)(u_i))}{\partial(x_j)}\right) = -\left(\frac{\partial p}{\partial(x_i)}\right) + \frac{\partial}{\partial(x_j)}\mu\left(\frac{\partial(u_i)}{\partial(x_j)} + \frac{\partial(u_j)}{\partial(x_i)}\right) - \left(\frac{2}{3}\right)\mu\left(\frac{\partial(u_k)}{\partial(x_k)}\right)(\delta_{ij}) + \rho(f_i) \quad (2)$$

Energy balance equation:

$$\left(\frac{\partial(\rho E)}{\partial t}\right) + \frac{\partial(\rho(Eu_j))}{\partial(x_j)} = -\frac{\partial(p(u_j))}{\partial(x_j)} + \frac{\partial(u_i)(\tau_{ji})}{\partial(x_j)} + \left(\frac{\partial}{\partial(x_j)}\left(K\frac{\partial(T)}{\partial(x_j)}\right)\right) + (S_E) \quad (3)$$

2.3

Where

- (f_i) is a force applied on the fluid
- (S_E) is the energy source term, and
- the tensor (τ_{ij}) is

$$(\tau_{ij}) = \mu\left(\frac{\partial(u_i)}{\partial(x_j)} + \frac{\partial(u_j)}{\partial(x_i)}\right) - \frac{2}{3}\mu\left(\frac{\partial(u_k)}{\partial(x_k)}\right) \quad (4)$$

Equations of state relate pressure $p = p(\rho, T)$ and internal energy $i = i(\rho, T)$ to the variables ρ and T . An example of this relation is the equation of state for an ideal gas:

$$p = \rho R T \quad (5)$$

3.2 Boundary Conditions

Boundary conditions are given in Table 2 and the density-based solver is used for the simulation.

Table 2: Initial Boundary Conditions

Parameter	Values
Inlet Pressure	691036.5 Pa
Inlet Temperature	300 K
Gauge Pressure	101325 Pa
Outlet Pressure	0 Pa
Outlet Temperature	300 K

3.4 Validation

The figure 3 represents the variation of temperature along the axial length of a Convergent–Divergent Nozzle and compares the results of the present study with the reference work conducted by S. A. Khan et al. (2021). The horizontal axis represents the nozzle length in meters, while the vertical axis indicates the temperature distribution in Kelvin. From the graph,

it can be observed that the temperature remains high at the inlet section of the nozzle, with values close to 300 K. As the flow moves through the converging section toward the throat region, the temperature gradually decreases due to the acceleration of compressible flow and conversion of thermal energy into kinetic energy. A sharp temperature drop is observed near the throat and divergent section, where the flow reaches supersonic velocity. The minimum temperature recorded is approximately 180–185 K around the middle section of the nozzle, indicating rapid expansion and strong cooling effects associated with high-speed compressible flow.

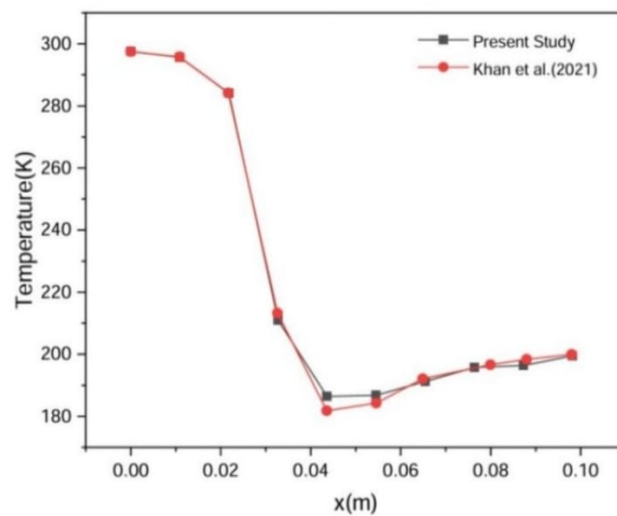


Figure 3: Plot of Temperature flow through the nozzle

Similarly, another graph of velocity flow through the nozzle is plotted for the same NPR, and a close agreement is found with the reference paper.

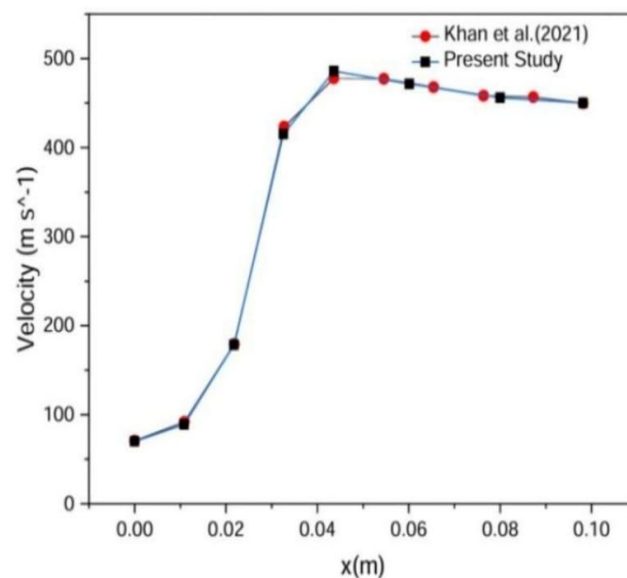


Figure 4: Plot of velocity flow through the nozzle

IV. RESULT AND DISCUSSION

Shock Visualization

4.1 Pressure Flows Contour

At NPR 6.82, the shock pattern is examined and Fig 5. The pressure contour shows the pressure distribution throughout the nozzles. The pressure gradually declines throughout the length of the nozzle, beginning with a maximum of approximately 667,628 Pa at the input and decreasing to a minimum of about 15,645 Pa at the output.

The transition is smooth, with the highest pressure concentrated in the converging section and a sharp drop near the throat. The expansion section shows a steady reduction in pressure, accompanied by periodic patterns resembling shock waves or pressure oscillations.

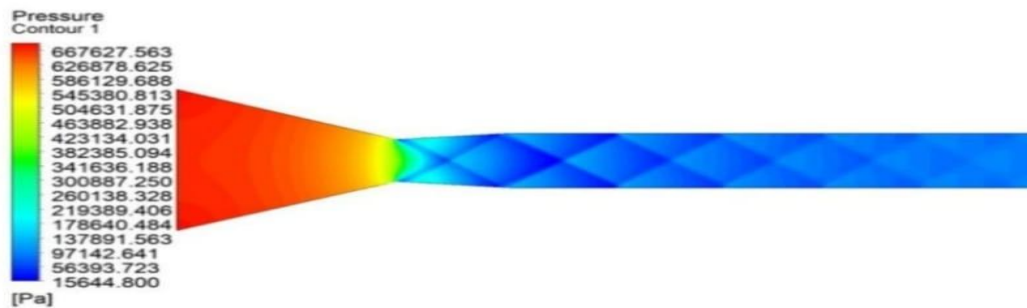
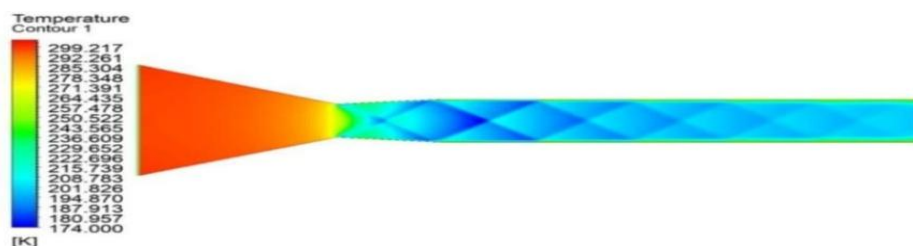


Figure 5: Contour of Pressure flow through the nozzle

The measured pressure distribution is consistent with the predicted behavior of fluid flow through a converging–diverging nozzle. The high inlet pressure correlates to the subsonic zone, when the fluid compresses as it moves toward the throat. The pressure at the throat drops to a minimum, indicating a critical flow situation in which the flow—speed approaches Mach 1. Beyond the throat, in the diverging portion, pressure oscillations are most likely owing to supersonic flow conditions and the formation of oblique shocks or expansion waves.

4.2 Temperature Flows Contour

The temperature distribution throughout the nozzle geometry shows a quick reduction from input to output. The temperature at the throat (narrowest part) drops dramatically due to the accelerated flow, which is dictated by the conservation of energy in flow that is compressible. The temperature stabilizes downwards of the nozzle, suggesting that heat transfer or energy loss has been decreased.



4.3 Density Flows Contour

The high-density area near the nozzle's converging portion shows subsonic flow with compressible properties. As the flow increases, the density at the throat (the narrowest part) decreases dramatically.

Downstream of the nozzle exit, periodic density changes are seen, which correspond to shock waves and expansion fans. The simulation depicts the behavior of compressible supersonic flow over a converging–diverging nozzle. The transition from subsonic to supersonic flow happens at the nozzle throat as a result of the choked-flow situation, when the Mach number is one.

Downstream of the nozzle exit, the periodic shock and expansion waves correspond to jet flow dynamics, in which—

The flow interacts with the ambient pressure.

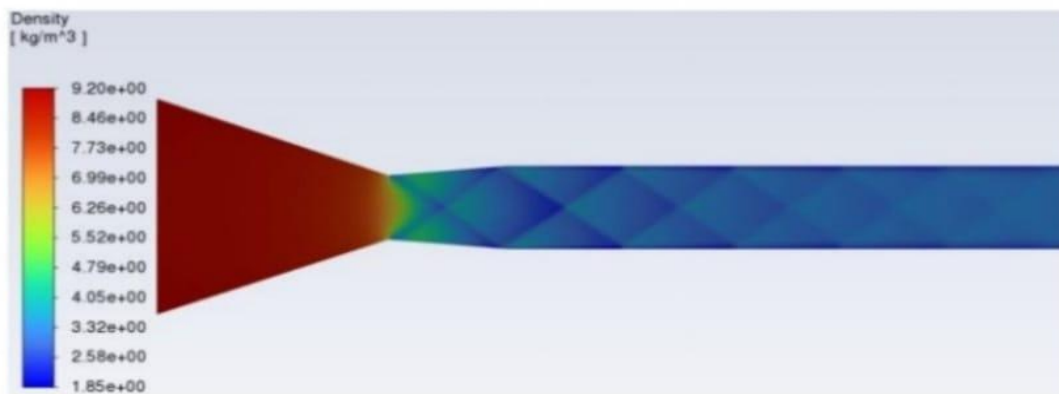


Figure 7: Contour of density flow through the nozzle

4.4 Velocity Flows Contour

A progressive rise in velocity between the intake and the nozzle throat. At a nozzle exit, the velocity peaks, indicating supersonic flow. The periodic densities and velocity changes beyond the nozzle are typical of a shock-cell pattern in supersonic jets.

These are caused by a mismatch between the jet's ambient pressure and exit pressure, resulting in compression and expansion waves.

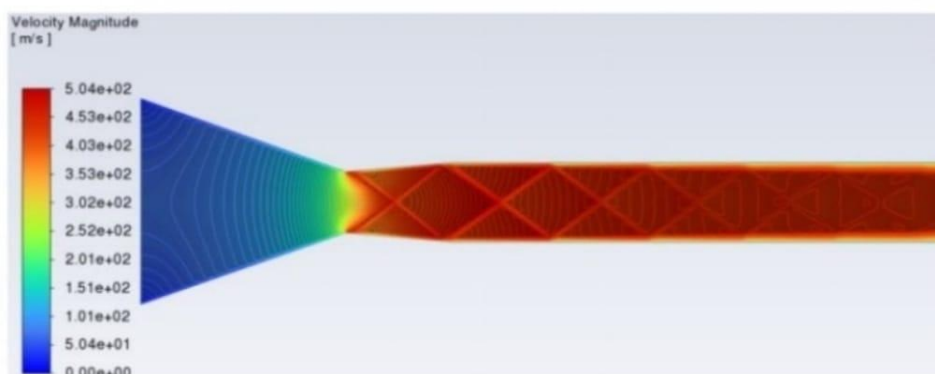


Figure 8: Contour of velocity flow through the nozzle

4.5 Under Expansion

To visualize the under-expansion shock, we have changed the geometry, keeping all the dimensions the same but the extended region is changed as shown in Fig. 9.

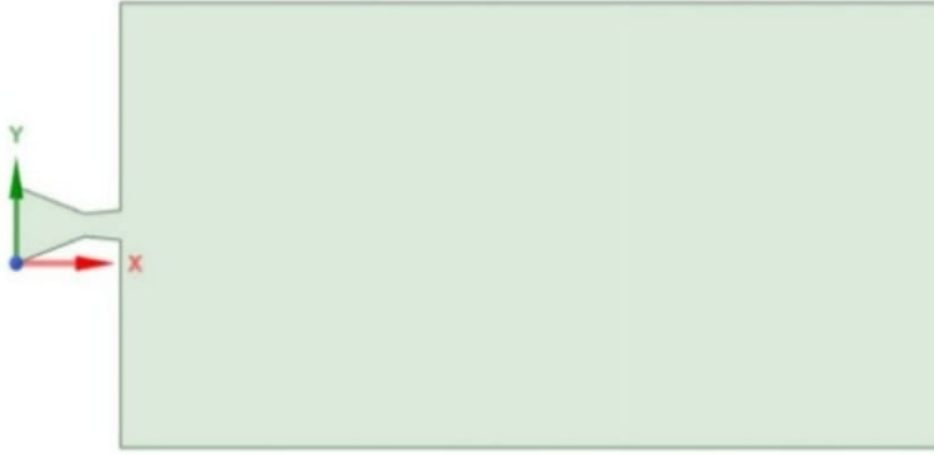


Figure 9: Two-dimensional CFD model of the C–D nozzle

We have used the same methodology and density-based solver to visualize the shock wave generated as shown in the velocity and temperature contour.

4.6 Under Expansion Contours

Contours showing changes in the density, velocity, and static temperatures illustrate how compressible, supersonic flow behaves via a converging–diverging nozzle in the simulation results.

As the flow accelerates from the intake to the throat, the density lowers more in the diverging portion. Periodic oscillations downstream show that the supersonic jet is interacting with shock–expansion waves. At the nozzle’s exit, where pressure differences with the surrounding environment cause the jet to form distinctive shock diamonds, the velocity increases gradually until it reaches its maximum.

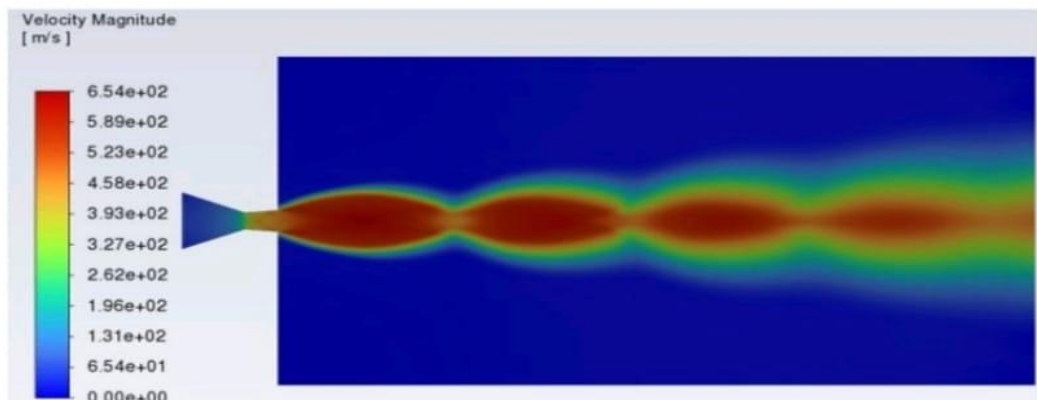


Figure 10: contour of velocity flow through the nozzle

As thermal energy is transformed into kinetic energy, static temperature contours exhibit a notable decrease, with alternate high and low temperature zones downstream signifying shock and expansion areas. These findings demonstrate how density, velocity, and temperature interact critically in supersonic flows.

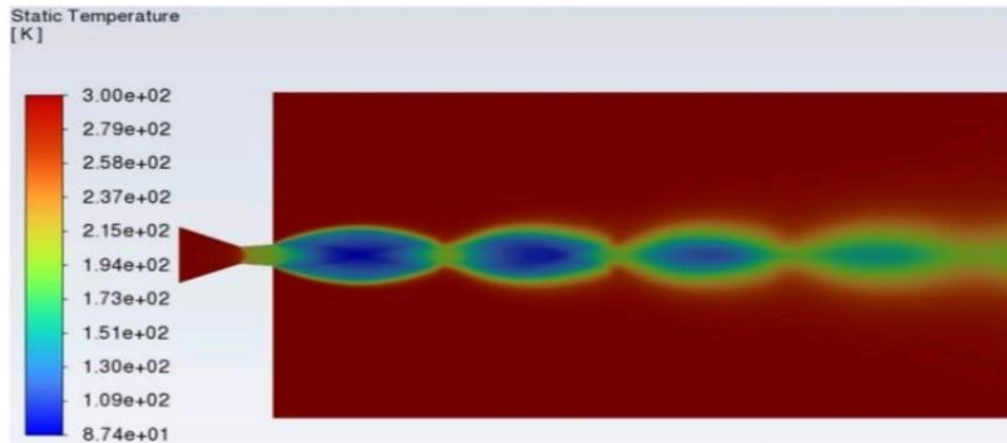


Figure 11: contour of Temperature flow through the nozzle

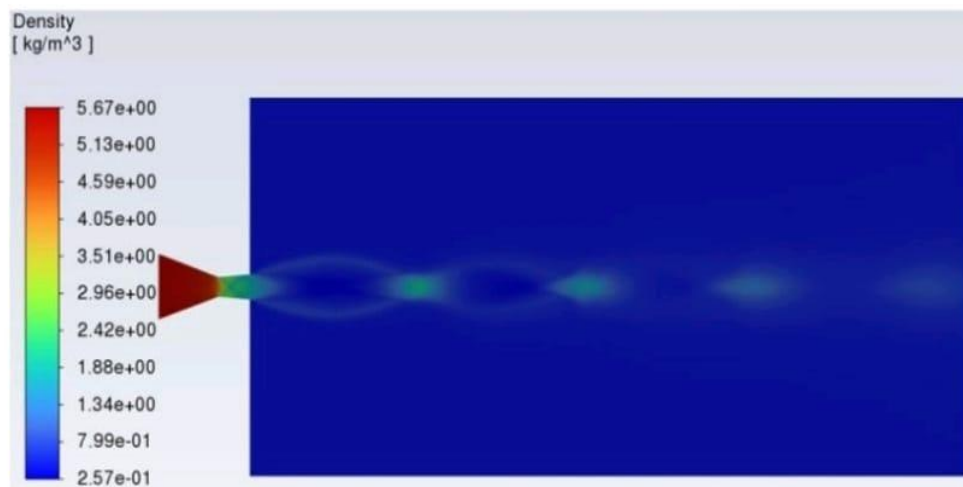


Figure 12: contour of Density flow through the nozzle

V. CONCLUSION

This work investigated the shock structures in a convergent-divergent nozzle under situations of underexpansion and overexpansion. In the overexpansion case it is found that a shock wave train forms inside the isolator zone, and the interaction of shocks is successfully simulated using CFD.

The obtained results from the overexpansion case could serve as benchmark data for simulations involving flow at Mach number of 2. Furthermore, pressure variations were effectively created by the shock train, which is an essential component for comprehending the behavior of supersonic flow. In the underexpansion case distinct diamond shock formed at the nozzle's exit due to pressure differences with the atmospheric conditions and the interaction between the shock and expansion wave through the converging diverging nozzle has been



successfully visualized. A significant drop in density was caused by the flow acceleration from the intake to the throat and across the diverging portion, and oscillating patterns downstream demonstrated how the supersonic jet and shock-expansion waves interacted. In velocity contour there is a gradual increase reaching at its maximum as thermal energy was transformed into kinetic energy. Whereas in Static temperature contour there is significant reduction in the downstream with a small increase in the expansion regions corresponding to the shock.

REFERENCES

- [1] V. Tapasvi, M. S. Gupta, and T. Kumaraswamy, "Designing and simulating compressible flow in a nozzle," *Int. J. Eng. Adv. Technol*, vol. 6, pp. 46-54, 2015.
- [2] E. Rathakrishnan, *Encyclopedia of fluid mechanics*. CRC Press, 2022.
- [3] G. Xu, K. D. Luxbacher, S. Ragab, J. Xu, and X. Ding, "Computational fluid dynamics applied to mining engineering: a review," *International Journal of Mining, Reclamation and Environment*, vol. 31, no. 4, pp. 251-275, 2017.
- [4] A. Aabid, S. A. Khan, M. A. A. Baig, and A. R. Reddy, "Investigation of flow growth in adduct flows for higher area ratio," in *IOP Conference Series: Materials Science and Engineering*, vol. 1057, no. 1. IOP Publishing, 2021, p. 012052.
- [5] A. Aabid and S. A. Khan, "Investigation of high-speed flow control from cd nozzle using design of experiments and cfd methods," *Arabian Journal for Science and Engineering*, vol. 46, no. 3, pp. 2201-2230, 2021.
- [6] A. Fluent et al., "Ansys fluent theory guide," Ansys Inc., USA, vol. 15317, pp. 724-746, 2011.
- [7] T. Al-Khalifah, A. Aabid, and S. A. Khan, "Regression analysis of flow parameters at high mach numbers," *Solid State Technol*, vol. 63, no. 6, pp. 5473-5488, 2020.
- [8] S. A. Khan, O. M. Ibrahim, and A. Aabid, "Cfd analysis of compressible flows in a convergent-divergent nozzle," *Materials Today: Proceedings*, vol. 46, pp. 2835-2842, 2021.